Damage classification of sandwich composites using acoustic emission technique and *k*-means genetic algorithm

Farzad Pashmforoush[1], Ramin Khamedi[2], Mohamad Fotouhi[1], Mehdi Ahmadi[1*]

[1.] *Non-destructive Testing Lab, Department of Mechanical Engineering, Amirkabir University of Technology, 424 Hafez Ave, 15914, Tehran, Iran.*

[2.] *Department of Mechanical Engineering, Zanjan University, Zanjan, Iran.*

[*] Corresponding author; Tel: (+98 21) 6454 3431; Fax: (+98 21) 8871 2838; Email address: Ahmadin@aut.ac.ir

ABSTRACT: In this study Acoustic Emission (AE) technique was used for monitoring mode I delamination test of sandwich composites. Since, during mode I delamination test various damage mechanisms appear, their classification is of major importance. Hence, integration of *k*-means algorithm and genetic algorithm was applied as an efficient clustering method to discriminate different failure modes. Performing primary experiments to find the relationship between AE parameters and damage mechanisms, the AE signals of obtained clusters were assigned to distinct damage mechanisms. Also, the dominance of damage mechanisms was determined based on the distribution of AE signals in different clusters. Finally SEM observation was employed to verify obtained results. The results indicate the efficiency of the proposed method in damage classification of sandwich composites.

KEY WORDS: Damage Mechanism, Sandwich Composite, Acoustic Emission, Clustering Analysis.

1. INTRODUCTION

Sandwich composites are widely used in a variety of engineering applications, including components of space vehicles, aircraft structures, marine vessels, train and truck structures, and containers and tanks. A sandwich is a special form of a laminated shell structure; consisting of three distinct layers that are bonded together to form an efficient load carrying assembly. Two thin face sheets of high performing material (fiber reinforced composite) are adhesively bonded

to each side of a thick but considerably lighter core (e.g. foam). The main benefits of using this particular lay-up are the high stiffness and strength to weight ratios, and greatly increased flexural strength and stiffness. Fiber reinforced composite sandwich materials are extensively used in structural applications mainly because of their relative advantages over other structural materials in terms of improved stability, weight savings, and ease of manufacture and repair [1]. Sandwich structures are often subjected to out-of-plane loading during utilization. In such cases, sandwich composites suffer severely by delamination cracking because of poor interlaminar fracture resistance. Due to the great effect of delamination on stiffness and long-term performance of composites, its detection is of great importance [2].

In order to perform online inspection of damage evolution in sandwich composites, AE technique has better applicability compared with other conventional non-destructive testing methods. Some advantages of AE method are online failure inspection, recognition and classification of damage mechanisms in real time [3-8]. Acoustic Emission (AE) is a robust non-destructive method for detection and recognition of different damage modes in composite materials. AE is a naturally occurring phenomenon, which is the result of transient elastic wave propagation caused by a sudden release of energy inside the material [9].

In composite materials there are various sources of AE signals such as matrix cracking, debonding, fiber breakage, etc. [7,8]. Therefore it is very important to discriminate AE signals corresponding to different failure mechanisms. In order to find the correlation between damage mechanisms and AE parameters, several studies have been carried out using different AE features such as counts, amplitude, energy [10, 11, 12]. Also, multi-parameter analysis has been used by several researchers to improve discrimination of AE events [13, 14, 15]. *K*-nearest algorithm is one of the supervised pattern recognition methods used by kenji and ono [16] for identification of damage modes in carbon /epoxy composites. Supervised pattern recognition is used whenever the number of damage mechanisms is known prior; While, unsupervised pattern recognition is performed without any previous knowledge. Unsupervised pattern recognition algorithm has been used by moevu et al. [17] in studying the AE signals of two SiCf/[Si–B–C] composites. The unsupervised algorithm could efficiently distinguish different types of matrix cracking.

Several researchers have used neural network for clustering AE signals [18, 19, 20]. Godin et al. [21] used integration of kohonen's self-organizing map and *k*-means algorithm to classify AE events of glass/epoxy composites and achieved interesting results. Kohonen's self-organizing

map, a neural network based approach, although accurate, suffers from high computational time. In addition, its performance is dependent on the network structure and number of neurons which must be specified prior [22]. Most of the above mentioned studies have been performed in time domain, while valuable information can be achieved using frequency domain. Wavelet transform is one the most suitable signal processing techniques in time-frequency domain that has been used by several researchers for analysing AE signals [23, 24]. The results indicate good performance of frequency analysis in studying AE events of composite materials.

In spite of various studies that have been performed on damage characterization of typical composites, there are a few studies on sandwich composites using AE technique. Until now, few researchers have used AE parameters to study the development of failure mechanisms in sandwich structures. Quispitupa et al. [25] have used AE waveform parameters such as amplitude and energy to study the damage mechanisms of the sandwich composites subjected to fatigue loading conditions. According to the obtained results, AE waveform parameters could classify damage mechanisms very well.

In this paper, hybrid of *k*-means algorithm and genetic algorithm was used to classify damage mechanisms during mode I delamination test. For this purpose, PCA was first used to reduce the dimensionality of rather large data. Then, integration of genetic algorithm and *k*-means algorithm was applied to cluster the data set. *K*-means algorithm is one of the most extensively used clustering methods, however, its performance strongly depends on the initial cluster centres and it may get stuck at local minima. In order to overcome this problem, GA was used as an efficient technique to find optimum cluster centres. Indeed, the searching capability of genetic algorithm can provide an optimal solution in a reasonable time.

After clustering analysis, mean AE parameters of each cluster were calculated and the best distinguished parameter was selected for damage characterization.

According to the primary experiments that were performed to find the relationship between the ranges of AE parameters and damage mechanisms, the AE signals of each cluster were assigned to a distinct damage mechanism. Also the dominance of damage mechanisms during mode I delamination was investigated based on the distribution of AE signals in different clusters. This investigation was combined with microscopic observations by SEM to verify the results. A concise explanation of damage classification procedure is shown in Figure 1.

Figure 1. A concise explanation of damage classification procedure

2. EXPRIMENTAL PROCEDURE

2.1. Description of the Materials

The experimental work was done on sandwich composite materials with glass fiber/epoxy as skin and polyethylene foam as core. Three specimens with different interface angles were manufactured in lab (Table 1).

Table 1. Lay-up of specimens

A hand lay-up method was followed by a 24 h vacuum bagging, set for all the specimens. Also, starter crack was created by inserting a Teflon film with a thickness of about 20 μm as an initial crack for the delamination test. After the vacuum bagging, the plates were placed in open air for 48 h. For ensuring excellent quality, the plates were examined using ultrasonic c-scan. The approved plates were then marked and cut on a band saw with a fine-toothed blade to obtain mode I opening test coupons (according to ASTM D5528). The specimen dimensions were 220×20 mm^2 and total nominal thickness was 5.5mm and foam thickness was 3mm for all specimens. The 20 mm width was essential to provide the AE sensor with enough area to create good coupling since the sensor diameter was 5 mm.

In this study, glass fibers, pure epoxy resin and pure polyethylene foam were used in the tensile test to determine the correlation among the AE results and fiber breakage, matrix cracking and core damage, respectively.

2.2. Test Method

Four samples were used for each test specimen. Figure 2 shows the bundle testing tab, clamping system of bundle, and AE sensors.

The DCB (Double Cantilever Beam) shown in Figure 2 consists of a rectangular, uniform thickness, sandwich composite specimen, containing a non-adhesive insert on the mid-plane which serves as a delamination initiator. Opening forces were applied to the DCB specimen by means of loading hinges bonded to one end of the specimen. The ends of the DCB were opened by controlling displacement, while the load and delamination length were recorded.

Figure 2. Experimental set-up of mode I delamination test

The applied load versus opening displacement was recorded and stored digitally and post processed. Instantaneous delamination front locations are marked on the chart at intervals of delamination growth based on ASTM D5528 [26].

2.3. Testing device

A properly calibrated test machine was used which was operated in a displacement control mode with a constant displacement rate in the range from 0.5 to 500 mm/min. All the specimens were loaded in 2 mm/min. The testing machine was applied with grips to hold the loading hinges that were bonded to the specimen.

The acoustic emission software AEWin and a data acquisition system (PAC) PCI-2 with a maximum sampling rate of 40 MHz were used for recording AE events. A broadband, resonant-type, single-crystal piezoelectric transducer from Physical Acoustics Corporation (PAC), called PICO, was used as the AE sensor. The sensor had a resonance frequency of 513.28 kHz, and an optimum operating range of 100–750 kHz. The surface of the sensor was covered with grease in order to provide good acoustic coupling between the specimen and the sensor. The signal was detected by the sensor and enhanced by a 2/4/6-AST pre-amplifier. The gain selector of the preamplifier was set to 40 dB. The test sampling rate was 1 MHz and 16 bits of resolution, between 10 and 100 dB. Preliminary to damage check, the data acquisition system had been calibrated for each kind of specimens, according to a pencil lead break procedure. Then, a repeatable acoustic wave was generated in the specimen by a lead breakage on its surface. At the same time, the attenuation of the AE waves was measured. For this purpose, the lead breakage test was repeated several times and at different locations between the sensors. After the calibration step, AE signals were recorded during mechanical testing. Signal descriptors such as amplitude, duration, rise time, counts, and energy were calculated by the AE software (AEWin). During the test, two sensors were placed in a linear configuration located at a distance of 50 mm, as shown in Figure 2. Two sensors were used to ensure that only the AE signals of damage area were used for clustering analysis.

3. Clustering Analysis

3.1. Principal Component Analysis (PCA)

PCA is a multivariate analysis tool usually used to reduce dimensionality of a large data set to enable better visualization and analysis of data [27]. With the aim of dimensional reduction, the data is transformed to a new set of uncorrelated variables, i.e. the principal components. In fact, PCA projects the data along the directions that depict maximum variance in the data set. These directions are specified by the eigenvectors of the covariance matrix with the highest eigenvalues. Let x be the $n \times m$ input data set, where n and m are the number of AE signals and related variables (features) respectively. Since the variables don't have same units, the data has to be standardized. Standardization is achieved by transforming all data to have zero mean and unit standard deviation. In this case all variables have same weight. After data standardization, the covariance matrix is calculated. Then, eigenvectors and corresponding eigenvalues for covariance matrix have to be calculated. If C denotes the covariance matrix, the eigenvalues λ_i can be obtained by solving the determinant equation $det(C-\lambda_i)=0$. Then eigenvectors are columns of the matrix A such that $C=ADA^T$, where

$$D = \begin{bmatrix} \lambda_1 & 0 & \dots & 0 \\ 0 & \lambda_2 & \dots & 0 \\ \vdots & \vdots & \vdots & \vdots \\ 0 & 0 & \dots & \lambda_m \end{bmatrix} \quad (1)$$

Where, $\lambda_1 \geq \lambda_2 \geq \ldots \geq \lambda_m$.

Keeping only the first l eigenvectors for clustering analysis, the transformation to principal components is expressed as:

$$y = XA_l \quad (2)$$

3.2. *K*-means Algorithm

The task of k-means algorithm is to classify a set of n data points in m-dimensional space into k number of classes [28]. The classification procedure is done by minimizing the sum of squares of distances between the data and the relevant cluster centres. The first step of k-means algorithm is

to partition the input data into *k* initial clusters. After calculating the mean point of each cluster as the centre of the cluster, a new partition is created by assigning each point to the cluster with the nearest centre. For the new clusters, the new centroids are recalculated and the algorithm is repeated by alternate application of these two steps until the coordinates of cluster centres do not change any more. Since the number of clusters is not known a priori, the algorithm has to be executed with different values of *k* and the best partitioning must be defined by means of a validity criterion such as the Davis-Bouldin (DB) index [29]. The DB validity index is calculated as follows:

$$DB = \frac{1}{k}\sum_{i=1}^{k}\max_{i\neq j}\left\{\frac{s_i + s_j}{d_{ij}}\right\} \qquad (3)$$

Where *s* is the within-cluster distance, *d* the between clusters distance and *k* is the number of clusters. Low values of DB indicate good clustering.

3.3. *K*-means Genetic Algorithm

The most important disadvantage of *k*-means algorithm is that its performance strongly depends on the choice of the initial cluster centres and it usually gets stuck at local minima. In order to solve this problem, hybrid of *k*-means algorithm and genetic algorithm is proposed as an efficient clustering technique [30, 31]. In fact, integration of these algorithms – which makes a right balance between local exploitation and global exploration - can be a robust method for optimum clustering of AE events.

Before explaining the steps of *k*-means genetic algorithm, the type of chromosome representation should be clarified. In this study, each chromosome is represented as a series of real numbers expressing the cluster centres. The steps of the hybrid algorithm are as follows:

Step 1) Population initialization

K random points are chosen from input data set as the centres of clusters.

Step 2) Clustering

In this step, each point *x* is assigned to the cluster with nearest centre and then new centres are calculated by Equation 4:

$$z_i^* = \frac{1}{n_i} \sum_{x_j \in C_i} x_j, \ i = 1, 2, ..., k \quad (4)$$

Where, z_i^* is the new cluster centre and n_i is the number of points belonging to cluster C_i.

Step 3) Fitness computation

Fitness function is described as the summation of the Euclidean distances of the points from their corresponding cluster centres (Equation 5):

$$Fitness\ value = \sum_{i=1}^{k} \sum_{x_j \in C_i} \| x_j - z_i \| \quad (5)$$

Where, z_i denotes cluster centre and k is the number of clusters. For optimum clustering, fitness value must be minimized.

Step 4) Selection

According to fitness values, two parents are selected from a population to create two new children. In this study, Roulette wheel selection with elitist selection was used. Since elitist selection copies at least one best solution without any changes to a new population, it guaranties the best solution ever found to survive to end.

Step 5) Crossover

After selection is performed, two parents exchange their information to create new children with a specified crossover probability.

Step 6) Mutation

In this step, mutation takes place according to the Equation 6:

$$r' = \begin{cases} r \times (1 \pm 2\Delta) & if\ r \neq 0 \\ (\pm 2\Delta) & if\ r = 0 \end{cases} \quad (6)$$

Where r is the value at a gene position before mutation, r' after mutation and Δ is a number in the range [0, 1] generated with uniform distribution. The (+) or (-) sign both have same possibility to occur.

Step 7) Checking stopping criterion

The algorithm should be repeated while the stopping criterion is met. In this paper maximum number of iterations was used as stopping criterion.

Table 2 summarizes the initial parameters of KGA. Also, the flowchart of the algorithm is shown in Figure. 3.

Table 2. Initial parameters of KGA

Figure 3. Flowchart of KGA

4. RESULTS AND DISCUTION

In order to find the relationship between AE parameters and damage mechanisms, AE monitoring of pure failures (core failure, failure of the adhesive bond, matrix cracking, and fiber breakage) was used to create an AE reference pattern. Based on AE analysis of the test results, these failures were classified according to distribution of AE amplitude, energy and frequency. Table 3 summarizes AE characteristics of pure damage modes. Applying Fourier Transform (FFT), the frequency distribution versus power spectrum was obtained as shown in Figure 4. According to the obtained results from pure failures (Table 3), there is some overlap between AE amplitude and energy ranges; whereas, the dominant frequency range of signals related to different failures varies significantly. The different frequency pattern of pure failure modes is an important key in damage classification procedure. According to the results the highest frequencies are associated with fiber breakage and the lowest ones are related to core failure. The frequency ranges of adhesive failure and matrix cracking are between core failure and fiber breakage frequency ranges.

Table 3. AE characteristics of pure failure modes

Figure 4. Frequency distribution vs. power spectrum: a) core failure, b) failure of the adhesive bond, c) matrix cracking, d) fiber breakage

After determining the correlation between AE parameters and damage mechanisms, mode I delamination tests were carried out and the AE signals were recorded. In order to cluster AE events, PCA was first used to reduce the dimensionality of rather large data set and to visualize

the results in a two-dimensional subspace. Since the selected AE parameters weren't in similar units, standardization of these parameters was done by means of their standard deviation.
After dimensional reduction, the AE signals were clustered using *k*-means genetic algorithm. The optimum number of clusters was calculated using Davis-Bouldin validity index. For this purpose, the hybrid algorithm was executed with values of k from 2 to 10 and DB index was calculated for each run. Figures 5-7 illustrate average DB index versus number of clusters (k). According to these figures the optimum number of clusters which minimizes the DB index is four. Hence, four damage mechanisms are expectable during mode I delamination test.

Figure 5. Davis-Bouldin validity index versus number of clusters in specimen S1
Figure 6. Davis-Bouldin validity index versus number of clusters in specimen S2
Figure 7. Davis-Bouldin validity index versus number of clusters in specimen S3

Figures 8-10 show frequency content of clustered AE signals versus amplitude. The dominant ranges of other AE parameters are listed in Table 4. The results indicate that among different AE descriptors, frequency is the best distinguished parameter; hence it can be used as an efficient AE parameter for damage classification of sandwich composites.

Figure 8. Frequency – amplitude plot of clustered AE signals in specimen S1
Figure 9. Frequency – amplitude plot of clustered AE signals in specimen S2
Figure 10. Frequency – amplitude plot of clustered AE signals in specimen S3

Table 4. Dominant ranges of AE parameters

According to the results of primary experiments conducted on pure failure modes (Table 3), the AE signals of each cluster could be assigned to a different damage mechanism. Although there are some differences between pure failure results and mode I delmaintion results, the most important point is the relationship between frequency range and damage mechanisms. As mentioned above, the highest and the lowest frequency ranges are representatives of fiber breakage and core failure, respectively. Meanwhile, the frequency ranges of adhesion failure and matrix cracking are between core failure and fiber breakage frequency ranges. Considering this relationship, the AE signals of the first cluster are associated with core failure, the second cluster

with adhesion failure, the third cluster with matrix cracking and the forth cluster with fiber breakage.

Also, the dominance of damage mechanisms was determined according to the distribution of AE signals in different clusters, as summarized in Table 5.

Table 5. Dominance of damage mechanisms

Hence it can be concluded that, core failure and fiber breakage are the most dominant failure modes in specimen S1. These two damage modes contain 65% of total AE events. However, there is some matrix cracking (about 20%). In this specimen, due to appropriate adhesion between core and skin, debonding is not noticeable. Only 15% of AE signals are related to this kind of damage mechanism. Although failure of the adhesive bond is negligible in specimen S1, it is the most prevailing damage mode in specimens S2 and S3. Adhesion failure contains 35% and 45% of total AE events of specimens S2 and S3, respectively. The second significant damage type in specimen S2 is core failure, while for specimen S3 core failure involves only 15% of AE events. In specimen S3 matrix cracking is more dominant as well as adhesion failure.

SEM observations of damage mechanisms are illustrated in Figures 11-13. The figures show dominant damage modes in different interfaces. The results are in good consistence with k-means genetic algorithm results.

Figure 11. SEM observation of damage mechanisms in specimen S1

Figure 12. SEM observation of damage mechanisms in specimen S2

Figure 13. SEM observation of damage mechanisms in specimen S3

5. CONCLUSION

During mode I delamination test of sandwich composites various damage mechanisms appear. Identification and classification of these damage mechanisms is an important task that was studied in this paper. For this purpose, Acoustic Emission technique was used as an efficient non-destructive testing method. In order to cluster AE signals generated during mode I delamination test, integration of *k*-means algorithm and genetic algorithm was applied. Based on the relationship between AE events and damage mechanisms, the AE signals were assigned to distinct damage mechanisms. Among different AE parameters, frequency was the best

distinguished descriptor to characterize damage modes. It was found that frequency ranges of 35-65, 100-130, 170-250 and 350-450 kHz were concerned with the core failure, failure of adhesive bond, matrix cracking and fiber breakage, respectively. Considering the distribution of AE signals in different clusters, the dominance of damage mechanisms was achieved for each of the layups. It was found that core failure and fiber breakage were the most prevailing failure mechanisms in specimen S1; while adhesion failure and core failure were more dominant in specimen S2. For specimen S3 adhesion failure and matrix cracking were the most important damage mechanisms. SEM observations were consistent with these results. The results show that AE technique accompanied by clustering algorithms can be promising methods for identification and classification of damage mechanisms in sandwich composites.

ACKNOWLEDGMENT

The authors wish to thank the Department of Mechanical Engineering at Amirkabir University of Technology, for providing the facilities for this study.

REFRENCES

[1] Belingardi G., Cavatorta MP., Duella R.,: Material characterization of a composite–foam sandwich for the front structure of a high speed train. Composite Structures, **61**(1-2), 13-25 (2003).

Doi:10.1016/S0263-8223(03)00028-X

[2] Pagano NJ., Schoeppner GA.: Delamination of polymer matrix composites: Problems and Assessment. (ed(s).: Kelly A. and Zweben C.) Comprehensive Composite Materials, 433-528 (2000).

[3] Bakukas J., Prosser W., Johnson W.: Monitoring damage growth in titanium matrix composites using acoustic emission. Composite Materials, **28**(4), 305–28 (1994).

Doi: 10.1177/002199839402800402

[4] Hajikhani M., Oskouei AR., Ahmadi M., Sharifi A., Heidari M.: Progressive Fracture Evaluation in Composite Materials by Acoustic Emission Technique. Key Engineering Materials, **465**, 535-538 (2011).

Doi: 10.4028/www.scientific.net/KEM.465.535

[5] Siron O., Chollon G., Tsuda H., Yamauchi H., Maeda K., Kosaka K.: Microstructural and Mechanical Properties of Filler-added Coal-tar pitch-based C/C Composites: the Damage and Fracture Process in Correlation with AE Waveform Parameters. Journal of Carbon, **38**, 1369-1389 (2000).
Doi: 10.1016/S0008-6223(99)00270-5
[6] Oskouei AR., Ahmadi M., Hajikhani M.: Wavelet-based acoustic emission characterization of damage mechanism in composite materials under mode I delamination at different interfaces. eXPRESS Polymer Letters, **3**(12), 804–13 (2009).
DOI: 10.3144/expresspolymlett.2009.99
[7] Ely TM., Hill EK.: longitudinal splitting and fibre breakage characterization in graphite epoxy using acoustic emission data. NDT&E International, **30**(2), 109-109 (1997).
Doi: 10.1016/S0963-8695(97)85524-7
[8] Uenoya T.: Acoustic emission analysis on interfacial fracture of laminated fabric polymer matrix composite. Journal of Acoustic Emission, **13**, 95-102 (1995).
[9] Ronnie K.M. Handbook of Nondestructive Testing, vol.5 Acoustic Emission. 2nd ed., American Society for Nondestructive Testing, (1987).
[10] Morscher GN., Martinez-Fernandez J., Purdy MJ.: Determination of interfacial properties using a single-fiber microcomposite test. Journal of the American Ceramic Society, **79**(4), 1083–91 (1996).
DOI: 10.1111/j.1151-2916.1996.tb08551.x
[11] Barré S., Benzeggagh ML.: On the use of acoustic emission to investigate damage mechanisms in glass-fibre-reinforced poly-propylene. Composites Science and Technology, **52**(3), 369-376 (1994).
Doi: 10.1016/0266-3538(94)90171-6
[12] Ativitavas N., Fowler T., Pothisiri T.: Acoustic emission characteristics of pultruded fiber reinforced plastics under uniaxial tensile stress, 'Proceeding of European WG on AE, Berlin, Germany', 447-454 (2004).
[13] Yamaguchi K., Oyaizu H., Johkaji J., Kobayashi Y.: Acoustic Emission technology using multi-parameter analysis of waveform and application to GFRP tensile tests. Acoustic Emission, current practice and future directions, ASTM STP 1077, Philadelphia, PA, 123-143 (1991).

[14] Pappas YZ., Markopoulos YP., Kostopoulos V.: Failure mechanisms analysis of 2D carbon/carbon using acoustic emission monitoring. NDT&E International, **31**(3), 157-163 (1998).
Doi: 10.1016/S0963-8695(98)00002-4
[15] Kostopoulos V., Loutas TH., Kontsos A., Sotiriadis G., Pappas YZ.: On the identification of the failure mechanisms in oxide/oxide composites using acoustic emission. NDT&E International, **36**(8), 571-580 (2003).
Doi: 10.1016/S0963-8695(03)00068-9
[16] Kenji K., Ono K. Pattern recognition of acoustic emission signals from carbon fiber/epoxy composites, 'Proceeding of 7th international acoustic emission symposium, Zao, Japan', (1987).
[17] Moevus M., Godin N., R'Mili M., Rouby D., Reynaud P., Fantozzi G., Farizy G.: Analysis of damage mechanisms and associated acoustic emission in two SiCf/[Si–B–C] composites exhibiting different tensile behaviours. Part II: Unsupervised acoustic emission data clustering. Composites Science and Technology, **68**(6), 1258–1265 (2008).
Doi: 10.1016/j.compscitech.2007.12.002
[18] Yan T., Holford K., Carter D., Brandon J.: Classification of acoustic emission signatures using a self-organization neural network. Journal of Acoustic Emission, **17**(1/2), 49-59 (1999).
[19] De Oliveira R., Marques AT.: Health monitoring of FRP using acoustic emission and artificial neural networks. Computers and Structures, **86**(3-5), 367-373 (2008).
Doi: 10.1016/j.compstruc.2007.02.015
[20] Philippidis TP., Nikolaidis VN., Anastassopoulos AA.: Damage characterization of carbon/carbon laminates using neural networks techniques on AE signals. NDT&E International, **31**(5), 329-40 (1998).
DOI: 10.1016/S0963-8695(98)00015-2
[21] Godin N., Huguet S., Gaeertner R.: Integration of the Kohonen's self-organizing map and k-means algorithm for the segmentation of the AE data collected during tensile tests on cross-ply composites. NDT&E International, **38**(4), 299-309 (2005).
Doi: 10.1016/j.ndteint.2004.09.006
[22] Haykin S: Neural Networks-A Comprehensive Foundation. 2nd ed., Macmillan College, New York, (1994).

[23] Ni QQ., Iwamoto M.: Wavelet transform of acoustic emission signals in failure of model composites. Engineering Fracture Mechanic, **69**(6), 717-728 (2002).
DOI: 10.1016/S0013-7944(01)00105-9
[24] Marec A., Thomas JH., El Guerjouma R.: Damage characterization of polymer-based composite materials: Multivariable analysis and wavelet transform for clustering acoustic emission data. Mechanical Systems and Signal Processing, **22**(6), 1441-1464 (2008).
Doi: 10.1016/j.ymssp.2007.11.029
[25] Quispitupa A., Shafiq B., Just F., Serrano D.: Acoustic emission based tensile characteristics of sandwich composites. Composites: Part B, **35** 563–571 (2004).
Doi: 10.1016/j.compositesb.2003.11.012
[26] ASTM Standard D5528: Standard Test Method for Mode I Interlaminar Fracture Toughness of Unidirectional Fiber-Reinforced Polymer Matrix Composites. ASTM International, West Conshohocken, PA, (2002).
[27] Jolliffe I.T: Principal Component Analysis. 2nd ed., springer series in statistics, (2002).
[28] Likas A., Vlassis N., Verbeek J.: The global k-means clustering algorithm. Pattern Recognition, **366**(2), 451-461 (2003).
Doi: 10.1016/S0031-3203(02)00060-2
[29] Davies DL., Bouldin DW.: A cluster separation measure. IEEE Transactions on Pattern Analysis and Machine Intelligence, **1**(4), 224-227 (1979).
Doi: 10.1109/TPAMI.1979.4766909
[30] Murthy CA., Chowdhury N.: In search of optimal clustering using genetic algorithms. Pattern Recognition Letters, **17**(8), 825-832 (1996).
Doi: 10.1016/0167-8655(96)00043-8
[31] Bandyopadhyay S., Maulik U.: An evolutionary technique based on *K*-Means algorithm for optimal clustering in RN. Information Science, **146**(1-4), 221-237 (2002).
Doi: 10.1016/S0020-0255(02)00208-6

List of figure captions:

List of table captions:

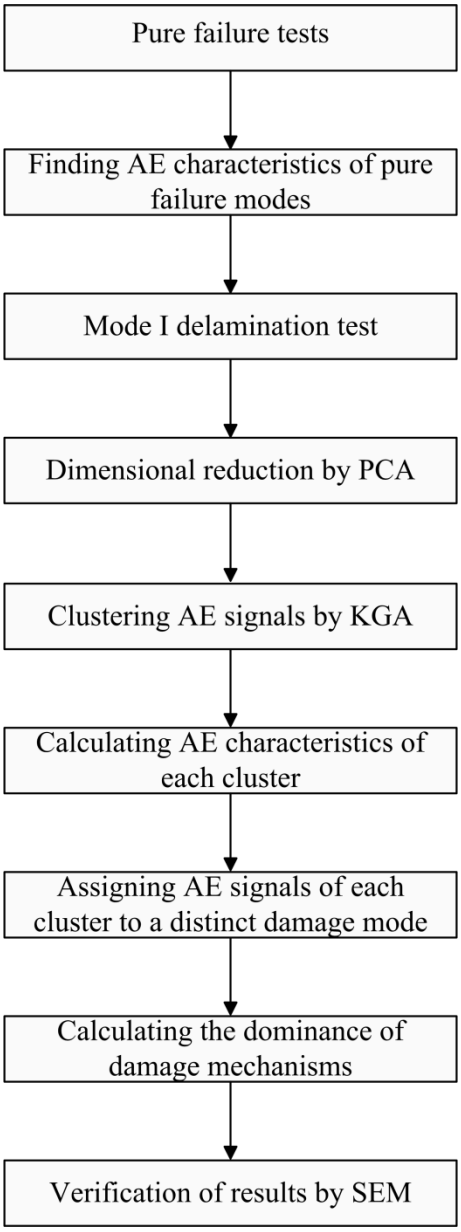

Figure 1. A concise explanation of damage classification procedure

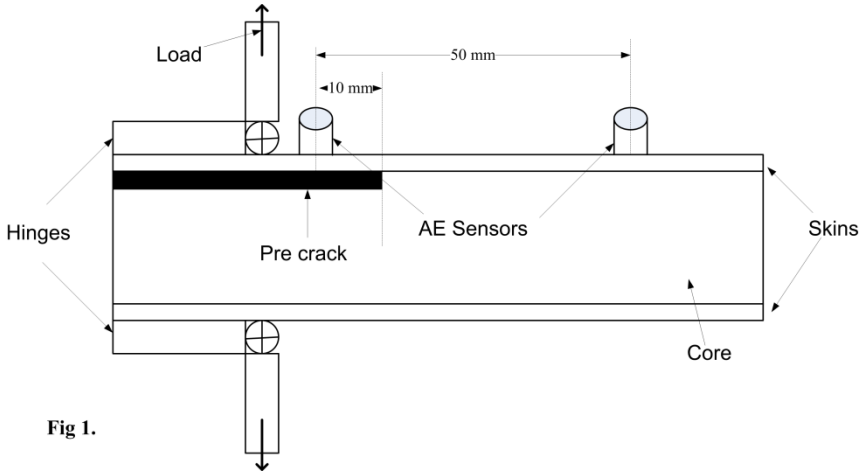

Figure 2. Experimental set-up of mode I delamination test

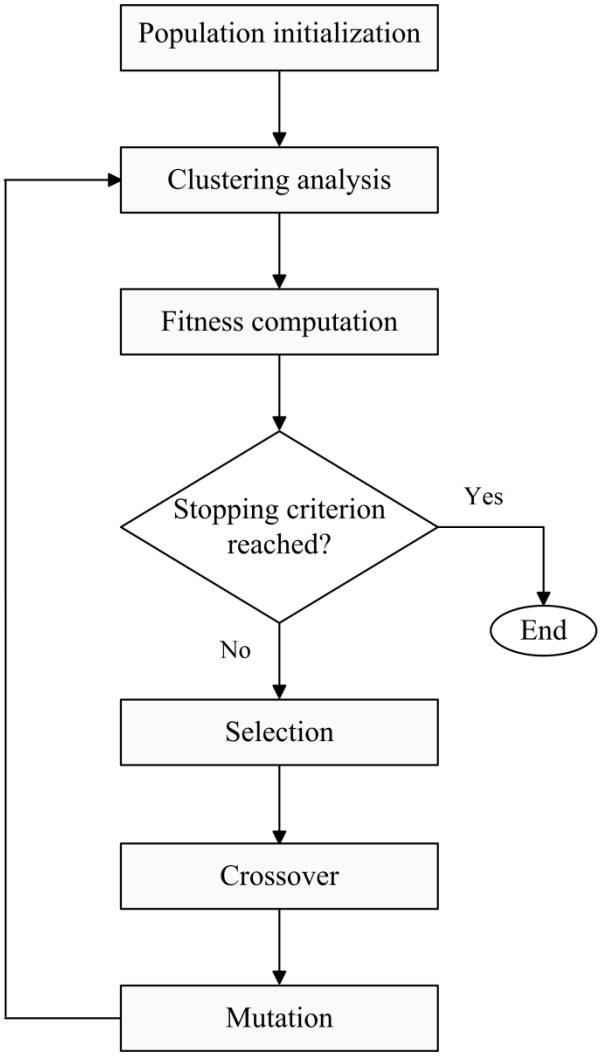

Figure 3. Flowchart of KGA

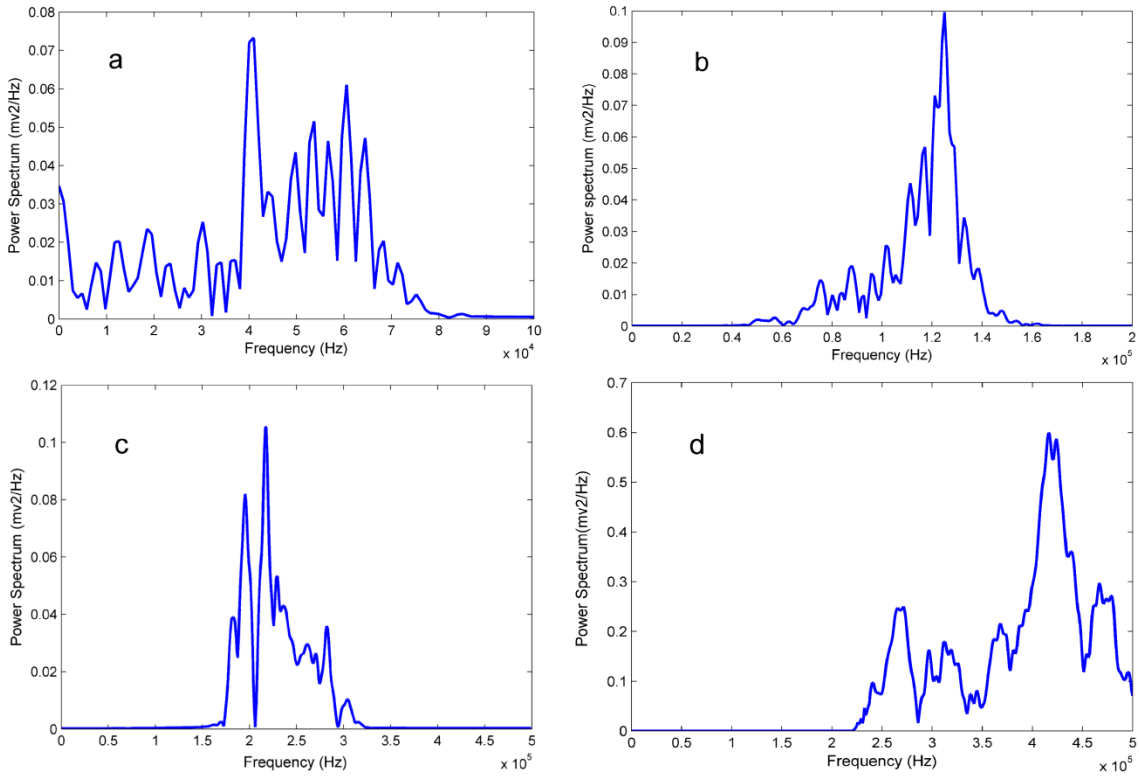

Figure 4. Frequency distribution vs. power spectrum: a) core failure, b) failure of the adhesive bond, c) matrix cracking, d) fiber breakage

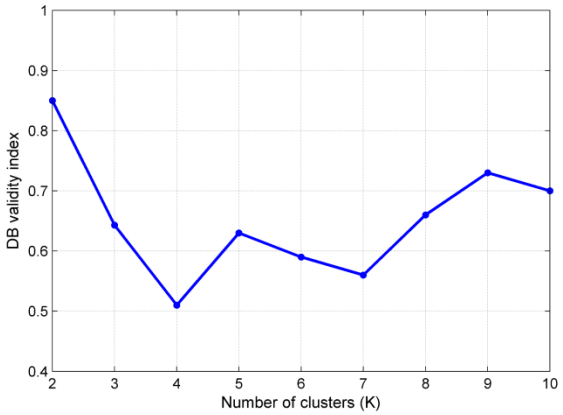

Figure 5. Davis-Bouldin validity index versus number of clusters in specimen S1

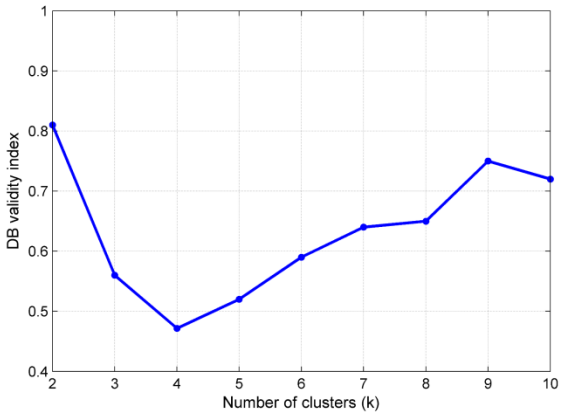

Figure 6. Davis-Bouldin validity index versus number of clusters in specimen S2

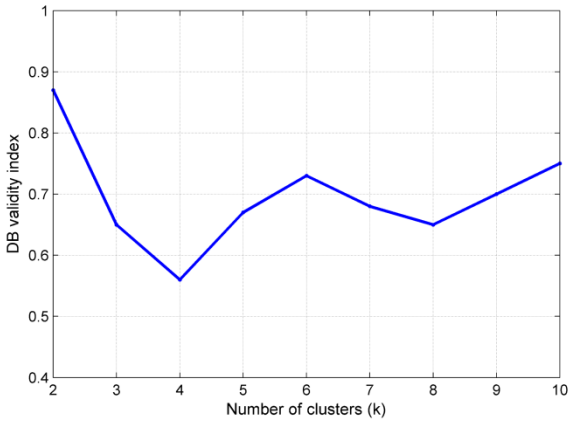

Figure 7. Davis-Bouldin validity index versus number of clusters in specimen S3

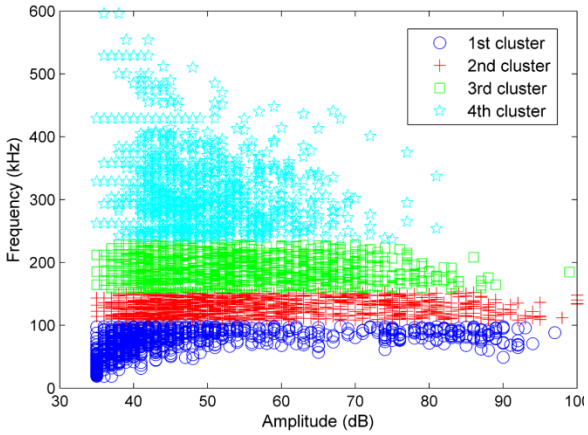

Figure 8. Frequency – amplitude plot of clustered AE signals in specimen S1

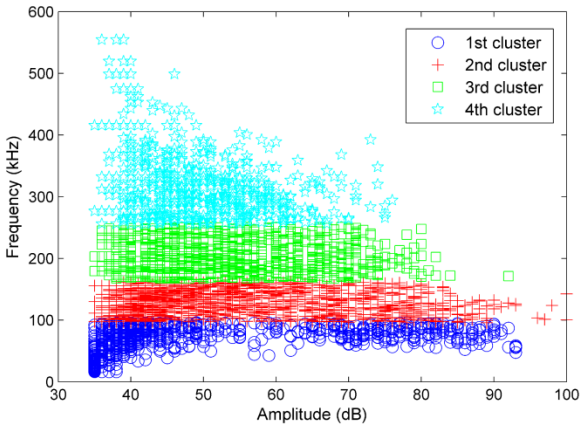

Figure 9. Frequency – amplitude plot of clustered AE signals in specimen S2

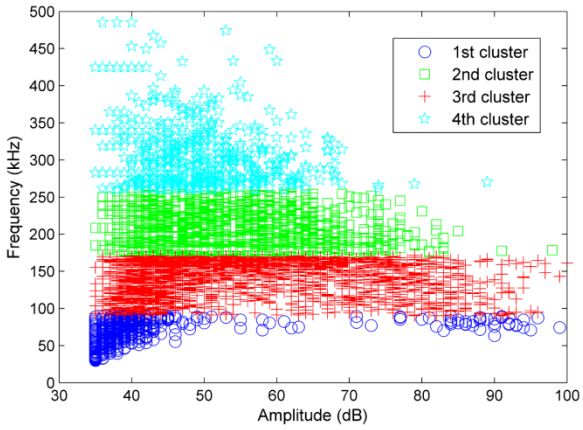

Figure 10. Frequency – amplitude plot of clustered AE signals in specimen S3

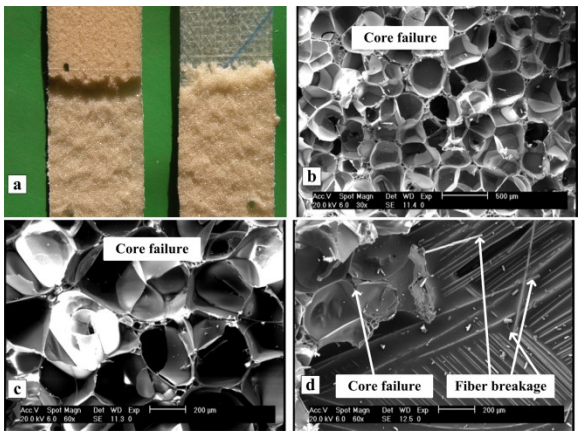

Figure 11. SEM observation of damage mechanisms in specimen S1

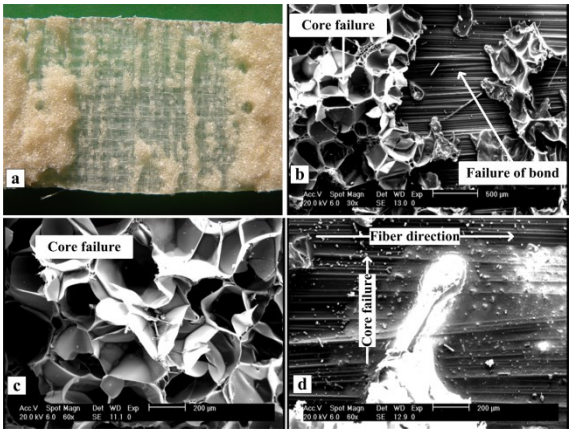

Figure 12. SEM observation of damage mechanisms in specimen S2

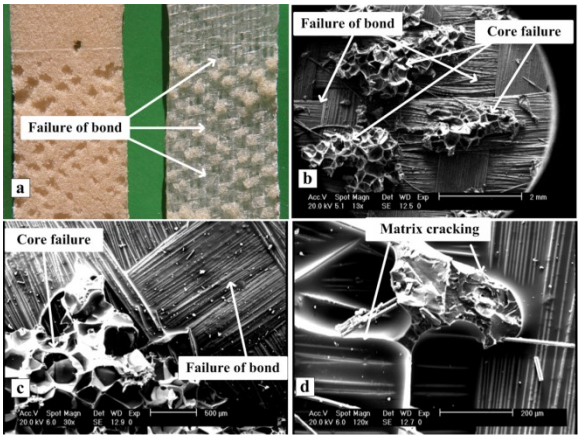

Figure 13. SEM observation of damage mechanisms in specimen S3

Table 1. Lay-up of specimens

No. of Specimens	**Interfaces**
S1	Woven (-45/45)/Foam
S2	90/Foam
S3	Woven (0/90)/Foam

Table 2. Initial parameters of KGA

Initial population	Crossover rate	Mutation rate	Maximum number of iterations
100	0.75	0.01	1000

Table 3. AE characteristics of pure failure modes

Failure mode	Dominant Amplitude ranges (dB)	Dominant Energy ranges (aj)	Dominant Frequency ranges (kHz)
Core Failure	40-60	0-30	30-80
Failure of the Adhesive Bond	60-80	5-230	100-150
Matrix Cracking	75-85	90-390	160-250
Fiber Breakage	85-105	350-1250	250-500

Table 4. Dominant ranges of AE parameters

Specimen	Dominant Amplitude range (dB)	Dominant Frequency range (kHz)	Dominant Count range	Dominant Duration range (μs)
S1	35-55 40-60 40-70 45-70	25-100 100-150 160-240 240-500	20-1500 10-550 5-250 5-40	25-10000 10-2400 5-1500 5-500
S2	35-50 40-60	30-95 100-160	20-1100 10-545	20-9100 15-5400

	40-65 45-65	170-250 250-500	5-265 5-35	10-2000 5-600
S3	35-45 40-65 40-70 45-70	35-90 95-170 170-255 260-450	25-560 15-560 5-250 5-40	10-6000 10-2100 5-1500 5-500

Table 5. Dominance of damage mechanisms

Specimen	Core Failure (%)	Failure of the Adhesive Bond (%)	Matrix Cracking (%)	Fiber Breakage (%)
S1	35	15	20	30
S2	30	35	25	10
S3	15	45	25	15